

# Novel *Dioscorea hispida* starch-based hydrogels and their beneficial use as disinfectants

Journal of Bioactive and  
Compatible Polymers

1–18

© The Author(s) 2015

Reprints and permissions:

sagepub.co.uk/journalsPermissions.nav

DOI: 10.1177/0883911515597704

jbc.sagepub.com



**Imran Azman<sup>1</sup>, Sahilah A Mutalib<sup>1</sup>,  
Siti Fairus M Yusoff<sup>1</sup>, Shazrul Fazry<sup>2</sup>,  
Akram Noordin<sup>2</sup>, Malina Kumaran<sup>2</sup> and  
Azwan Mat Lazim<sup>1</sup>**

## Abstract

Starch-grafted polyacrylamide hydrogels were successfully prepared via chemical polymerization method in basic solution, which provides a homogeneous suspension in the reaction system. The results obtained from Fourier transform infrared–attenuated total reflectance confirmed that the monomer polyacrylamide was grafted onto the starch backbone as shown by the cross-linked peak at  $1638\text{ cm}^{-1}$ . Scanning electron microscopy showed that the morphology of starch-grafted polyacrylamide hydrogels has a highly porous structure which provides excellent water absorption capacity with a swelling ratio up to 124%. The X-ray diffraction showed no significant crystallization peaks, indicating that an amorphous hydrogel has been produced. Supported by differential scanning calorimetry, the highest transition glass temperature was observed at  $101^\circ\text{C}$ . The starch-grafted polyacrylamide hydrogel extracts inhibited *Escherichia coli*, *Staphylococcus aureus*, *Saccharomyces cerevisiae*, and *Salmonella typhimurium* growth. The fish embryo toxicity test demonstrated that the hydrogel with 2:1 ratio of polyacrylamide: starch has an acceptable level of toxicity. This result indicates that the synthesized hydrogel is applicable for biological purposes with further modifications.

## Keywords

Hydrogel, dioscorine, starch, antibacteria, toxicity

<sup>1</sup>School of Chemical Sciences and Food Technology, Universiti Kebangsaan Malaysia, Bangi, Malaysia

<sup>2</sup>School of Biosciences and Biotechnology, Universiti Kebangsaan Malaysia, Bangi, Malaysia

## Corresponding author:

Azwan Mat Lazim, School of Chemical Sciences and Food Technology, Universiti Kebangsaan Malaysia, Bangi 43600, Selangor Darul Ehsan, Malaysia.

Email: azwanlazim@ukm.edu.my

## Introduction

Since its invention in the 1950s, hydrogels with antimicrobial activity have been widely used in biomedical applications, especially in wound dressing. In many reported cases, the infection was affected by bacteria or fungi such as *Escherichia coli*, *Staphylococcus aureus*, and *Aspergillus niger* and in severe cases have led to death. To overcome the problems, many innovations were made using several types of gels and resins with antibacterial and anti-fungal abilities.

Super-absorbent hydrogels are characterized by a polymeric cross-linked network with excellent hydrophilic capacity.<sup>1</sup> It can absorb water more than a thousand times its original weight and the swelling equilibrium is such that it can retain liquid even when the polymer is placed under some pressure.<sup>2</sup> Due to their superior properties in comparison with traditional water-absorbing materials, super-absorbent hydrogels have been widely used in agricultures, hygiene products, horticultures, drug delivery systems, and food storage, including biomedicines.<sup>3</sup> In fact, approximately up to 90% of super-absorbent hydrogels are used in disposable materials<sup>4</sup> where most of them are made of synthetic polymers. In previous research, an electroresponsive drug delivery system was developed using poly(acrylamide-grafted-xanthan gum) (PAam-g-XG) hydrogel for transdermal delivery of ketoprofen.<sup>5</sup> The membrane-controlled drug delivery systems were prepared using drug-loaded PAam-g-XG hydrogel as the reservoir and cross-linked with poly(vinyl alcohol) to form films as rate controlling membranes (RCMs). In addition, due to high possibility of absorbency, a novel kappa-carrageenan (C)-based super-absorbing hydrogel was synthesized through graft copolymerization of acrylamide (Aam) onto a C substrate in the presence of a cross-linking agent.<sup>6</sup>

Modified starch-based polymers can be engineered for specific properties by combining starch with synthetic polymers through a graft copolymerization process. There are many methods that have been established in preparing a starch-based hydrogel, such as conventional, batch processing, and extrusion. As an example, hydrogels made of starch–polyacrylamide (pAam)-grafted copolymers have received much attention due to their potential use in many applications such as super-absorbents,<sup>7,8</sup> paper-making additives,<sup>9,10</sup> drag reduction,<sup>11</sup> and textile sizing.<sup>12</sup>

Although the synthetic hydrogel is often demonstrated as being a good absorbent, it shows low levels of degradability and remains in the environment for prolonged periods.<sup>13</sup> As an example, conventional super-absorbents made of poly(sodium acrylate) are highly toxic as they attack important human organs such as the lungs, eyes, and skin once it is inhaled or ingested.<sup>14</sup> This biodegradability becomes a main factor for the super-absorbent hydrogel in terms of its eco-friendliness.<sup>15</sup>

As a by-product of grain crops, starch tubers are abundant bio-resources which contain 40%–60% of natural amylose and amylopectin. However, these wild yams have not been fully utilized.<sup>16</sup> One of them is *Dioscorea hispida* (locally known in Malaysia as Ubi Gadong), which is a poisonous plant that contains toxic poison in its rhizome. There are approximately over 600 *Dioscorea* species found in various parts of the world, especially in tropical and subtropical regions.<sup>17,18</sup> In contrast, *D. hispida* starchy tuber is edible and can be consumed after the poison (dioscorine) has been removed.<sup>19–21</sup> Traditionally, it takes 5–7 days of soaking the *D. hispida* tubers in flowing water for the detoxification process to complete before it is safe for human consumption.<sup>22,23</sup>

The majority of the literature has reported on the utilization of commercially available starch to synthesize hydrogels.<sup>24</sup> Moreover, in order to obtain antibacterial effects, the hydrogel is incorporated into an inorganic material such as silver nanoparticles<sup>25</sup> or by combining several chemicals.<sup>26</sup> To our knowledge, there has been no literature reported on the preparation of hydrogels based on the exotic wild yam, *D. hispida*. In addition, there have been no reports to demonstrate that starch-based hydrogel itself has any antibacterial properties.

This research explores the characteristics of the *D. hispida* starch-based hydrogel and investigates its resistance toward bacterial activity. A simple method has been used to prepare a super-absorbent starch-based hydrogel grafted with pAam.<sup>27</sup> The hydrogel was characterized to determine its optimum performance. The degree of swelling was determined for different hydrogel ratios while the characterization was made by using Fourier transform infrared (FTIR) spectroscopy, scanning electron microscope (SEM), and X-ray diffraction (XRD) analysis. The hydrogel was assayed using the disk diffusion susceptibility method to investigate antimicrobial properties. Further investigations were made on the toxicity properties of the synthesized hydrogels. Aqueous extractions of the hydrogels were tested on 1 h post-fertilization (hpf) zebrafish embryos. Both assays revealed that hydrogels possessed antimicrobial properties and acceptable biocompatibility.

## Materials and methods

### Materials

All chemicals used in this study were of analytical grade and solutions were prepared using distilled water. *D. hispida* yam was obtained from Terengganu, Malaysia. pAam (Sigma–Aldrich) was used without further purification. As for the cross-linking agent and initiator, *N,N'*-methylenebisacrylamide (MBA) (Merck) and potassium persulfate (KPS) (Merck) were used. A Denver 215 model pH meter and a Heidolph MR3001 model magnetic stirrer were used during the experiments. A Retsch PM200 model grinder was used to grind the starch compound into fine powder with a diameter of approximately 5 nm. A polyscience 9006 model refrigerating–heating circulator was also used during the starch-based hydrogel synthesis. This refrigerating–heating circulator was used to ensure that all chemical processes such as radical reactions and cross-linking polymerization were performed without any physical or chemical effects from the surroundings.

### Preparation of starch and starch stock solution

Past researchers have stated that *D. hispida* wild yam is a poisonous plant<sup>28,29</sup> due to its tuber containing toxic poison and can be consumed after the poison (dioscorine) is properly removed.<sup>20,21</sup> Due to traditional processing methods, the removal of dioscorine is difficult in practice. The tubers were peeled, sliced, and soaked in flowing water (river) for up to 7 days during the traditional detoxification process.<sup>30</sup> However, the toxic alkaloids (dioscorine) were left unfiltered in order to perform an antibacterial activity test. The wild yam tubers were peeled and rinsed before being ground using a home blender. The suspension was kept in a container and left overnight. After 24 h, the upper layer of the suspension was removed while the lower layer was collected and dried in the oven for 3 days. The dried starch was then ground down.

### Synthesis of *D. hispida* starch–pAam hydrogel

*D. hispida* starch (2 g) was mixed in 10 mL (5 w/v%) of sodium hydroxide solution with constant stirring (300 r/min) at room temperature for 1 h to form gelatinized starch mixtures. Later, the gelatinized starch mixtures were added to 0.25 g MBA and the initiator. The flasks were stoppered and the contents stirred and refluxed with monomer pAam at 60°C and 400 r/min. In order to establish cross-linking, nitrogen gas was flowed into the refluxing solution. This is to avoid the formation of bubbles in the casted hydrogels and also to enhance the cross-linking between the monomer and starch. The mixtures were then casted into Petri dishes and dried at room temperature. The

membranes obtained were half transparent and labeled with various ratios of monomer and starch, which were 1:2, 2:1, and 3:5, respectively.

### Characterization of the hydrogels

FTIR analysis was conducted to characterize hydrogel films using PerkinElmer Spectrum BX-II Model FTIR spectrophotometer. Samples were dried to a constant weight in an oven at 50°C for 24 h before being used, and certain peaks of the samples were recorded in the range 4000–400 cm<sup>-1</sup> with an average of 50 scans at a resolution of 4 cm<sup>-1</sup>.

The surface of the complexes was observed with an emission SEM. The samples were coated with a thin gold layer (two times, 40 mA, 60 s; approximately 30 nm) by a sputter coater unit (Balzers SCD 050 Sputter Coater; BAL-TEC) and surface topography was analyzed with a JEOL JSM 6300F SEM operated at an acceleration voltage of 5 kV.

The XRD patterns of the hydrogels were recorded with oriented mounts in a Philips X'Pert Pro X-ray diffractometer using radiation at 45 kV and 40 mA in the range of 0°C–60°C. In order to investigate the thermal properties of starch, pAam, and synthesized hydrogels, differential scanning calorimetry (DSC) analysis of the samples was carried out with PerkinElmer Diamond thermogravimetric (TG)/DSC analyzer. The work was carried out using aluminum pans under a dynamic nitrogen atmosphere in a temperature range of 25°C–600°C and a heating rate of 5°C/min.

### pH-dependent swelling behavior of the hydrogel

To investigate the swelling behavior of the hydrogels, the swelling equilibrium upon addition of pure water and citric acid–phosphate solutions of definite pH values (1, 7, and 13) was studied as previously suggested.<sup>31</sup> The dried samples were immersed in the solutions at room temperature and removed at intervals of 5 min, dried with filter paper, and weighed before being put back into the same solutions until it reached equilibrium.

The pH-dependent swelling behavior of the hydrogel was determined by swelling the dried hydrogel in the water until equilibrium was reached. The samples were then immersed into the citric acid–phosphate solutions of different pH values, respectively, and allowed to stand for a maximum of 2 h in each solution. The swelling ratios were calculated on a dry basis using equation (1), where  $Wh$  is the weight of the product after hydration and  $Wd$  is the weight of the dried product. The experiments were conducted in triplicate, and so the results are reported as an average

$$\text{Swelling ratio} = \frac{Wh - Wd}{Wd} \times 100 \quad (1)$$

### In vitro antimicrobial activities of the hydrogels

The antimicrobial activity of hydrogels was assayed by the disk diffusion susceptibility test according to the recommendation of the National Committee for Clinical Laboratory Standards (NCCLS).<sup>32</sup> The disk diffusion tests were conducted on Müller–Hinton agar plates for four different bacterial cultures: *E. coli* [ATCC 25922], *S. aureus* [ATCC 25923], *Salmonella typhi*. [ATCC 14028], and *Saccharomyces cerevisiae* [ATCC 9763]. Plates were dried at 35°C–36°C for about 30 min in an incubator before inoculation. Three to four freshly grown colonies of bacterial strains were inoculated into 25 mL of Müller–Hinton broth medium in a shaking water bath for 4–6 h until a turbidity of 0.5 McFarland (1 × 10<sup>8</sup> colony-forming unit (CFU)/mL) was reached. The final

inocula were adjusted to  $5 \times 10^5$  CFU/mL. The inoculum (50 mL) from the final inocula was applied to each agar plate and uniformly spread with a sterilized cotton spreader over the surface. Absorption of excess moisture was allowed to occur for 30 min before application of hydrogel disks (9 mm). Hydrogel disks were incubated at 37°C for 24 h for all the bacteria. The inhibition zone diameter (mm) surrounding each sample was investigated after 24-h incubation of hydrogel disks (12 mg/9 mm) onto agar plates at 37°C.

### *Toxicity test using zebrafish embryo test (fish embryo toxicity)*

**Embryo of zebrafish.** Embryos were obtained from Dr Syahida Ahmad, Department of Biochemistry, Faculty of Biotechnology and Biomolecular Sciences, Universiti Putra, Malaysia. Viable fertilized eggs were washed and maintained in E3 embryo media (5.03 mM NaCl, 0.17 mM KCl, 0.33 mM  $\text{CaCl}_2 \cdot 2\text{H}_2\text{O}$ , 0.33 mM  $\text{MgSO}_4 \cdot 2\text{H}_2\text{O}$ , and 0.1% (w/v) methylene blue) at constant room temperature.<sup>33</sup>

Fish embryo toxicity (FET) tests were performed as outlined in the Organisation for Economic Co-operation and Development (OECD) draft guidelines.<sup>34,35</sup> In short, 1 hpf embryos were separated in a single well into a 96-well plate and maintained in 180  $\mu\text{L}$  of E3 embryo media at room temperature; 20  $\mu\text{L}$  of hydrogel extract was added to each well and diluted by a factor of 10. Embryos were observed under light microscope at 4 $\times$  magnification at 48 and 72 hpf.

**pAam–starch hydrogel extracts.** The synthesized hydrogels (from section “Synthesis of *D. hispida* starch–pAam hydrogel”) were extracted to obtain the crude extracts before being diluted in several ratios of volume concentration. The hydrogels were cut approximately into a 1 cm  $\times$  1 cm square area and immersed for 24 h in 5 mL of distilled water. The extracts were prepared in three pAam–starch ratios which were 3:5, 1:2, and 2:1. The crude extracts were then diluted in several volumes of distilled water (100, 1000, and 10,000 mL) and the ratio volumes of stock extracts with distilled water were presented as undiluted (1:100, 1:1000, and 1:10,000 mL) for each of those pAam–starch hydrogel ratios. The solutions were then poured into the tank of zebrafish embryo with 20  $\mu\text{L}$  of hydrogel extract added in each well to dilute the solution by a factor of 10 until 10,000. Embryos were observed under light microscope at 4 $\times$  magnification at 48 and 72 hpf.

## **Results and discussion**

### *Synthesis of starch-grafted pAam hydrogels*

Figure 1 shows a proposed mechanism for the synthesis of starch-grafted polyacrylamide (S-g-pAam) hydrogels, where acrylic radical polymerization with starch is a chain reaction process<sup>25</sup> consisting of three main steps: initiation, propagation, and termination. First, hydroxyl free radicals are formed on the starch backbone, a process initiated by KPS. Then, the pAam monomer reacts with the hydroxyl free radicals resulting in propagating a new polymer chain (branch) that is covalently anchored to the starch. The free radical site is then transferred to the newly formed branch. Subsequently, more pAam monomers may covalently bind to the free radical sites of the branch. The propagation of the branch continues until termination occurs either by cross-linking of two growing starch chains with MBA or by a disproportionation mechanism.<sup>36,37</sup> Propagation and termination may also occur by a chain transfer to monomer, initiator, dead polymer, or impurities. This shows that starch plays a major role in the synthesis of S-g-pAam hydrogel adsorbent. First, it provides high-density hydroxyl groups. Second, starch serves as the backbone of hydrogel networks, which determines the mechanical properties and machinability of the hydrogel material.

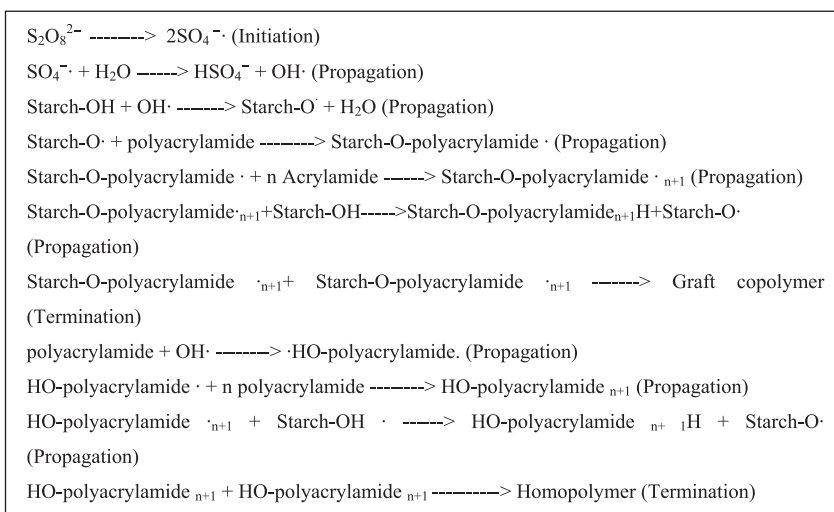


**Figure 1.** Proposed mechanism of biological synthesis of (S-g-pAam) hydrogels.

The starch and phosphoric acid solution provide a homogeneous reaction system and allow uniform and high substitution of starch derivatives.

## FTIR

FTIR spectra of the S-g-pAam hydrogels and the starch are shown in Figure 2. The starch and S-g-pAam hydrogel show absorption peaks at 3285.8 and 3287.04  $\text{cm}^{-1}$ , respectively, due to the hydrogen-bonded  $-OH$  groups of starch. Both show a peak around 2900  $\text{cm}^{-1}$  that corresponds to the  $-CH_2-$  asymmetric stretching of  $-CH_2OH$  groups in starch. For S-g-pAam hydrogels, a broad peak has appeared in the range of 1700–1642  $\text{cm}^{-1}$ , which is assigned to the  $C=O$  stretching vibration of  $-COOH$  groups of grafted pAam. Sharp peaks were observed at 1424 and 1415  $\text{cm}^{-1}$  in both pAam and S-g-pAam spectra and are due to the symmetric stretching of  $COO^-$  groups.<sup>38</sup> The peaks observed at 1700–1642 and 1415  $\text{cm}^{-1}$  prove the existence of carboxyl groups in the hydrogels after grafting polymerization. In comparison with the original starch, the FTIR spectrum of S-g-pAam hydrogels shows that the peak at 1075  $\text{cm}^{-1}$  for the  $C-O$  stretching vibration of  $-CH_2OH$  groups decreased in comparison with the peak at 1077  $\text{cm}^{-1}$  (starch). This result was insignificant, as it was previously reported<sup>39</sup> that the grafting polymerization reaction occurred in the primary hydroxyl groups of the starch. However, the existence of carboxyl groups is possibly also due to the blending of pAam monomer or its homopolymer not referring to the S-g-pAam hydrogels. Therefore, a thorough washing was performed by immersing the hydrogels in a 0.01 mol/L of NaOH for 2 days followed by freeze-drying. The NaOH-treated hydrogels exhibited similar FTIR characteristics as the untreated sample, which further confirmed that Aam was successfully grafted to cellulose instead of blending with cellulose.

## SEM

All characterizations of *D. hispida* starch have been reported in our previous research.<sup>31</sup> The SEM images in Figure 3 showed that a highly porous network structure with a maximum of 2  $\mu\text{m}$  was



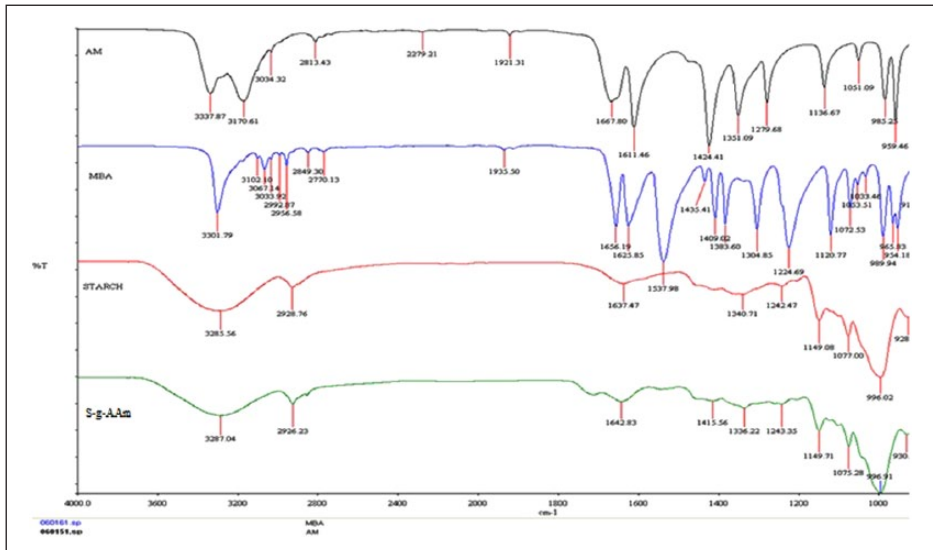


**Figure 2.** FTIR spectra of pAam monomer (AM), cross-linked agent (MBA), starch (comonomer), and grafted hydrogel ratio (S-g-pAam).

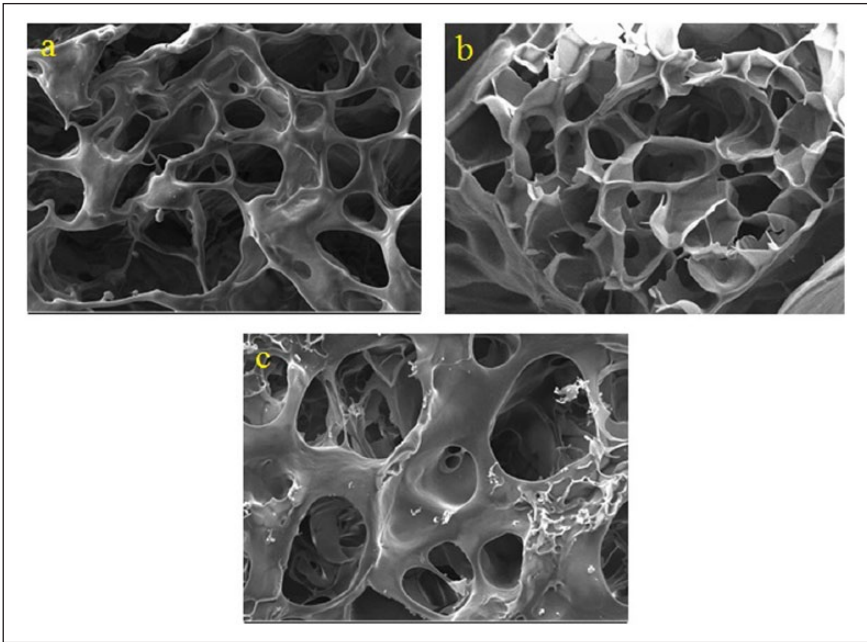


**Figure 3.** SEM micrographs at 100× magnification (2 μm) of three pAam:starch ratios: (a) 3:5, (b) 2:1, and (c) 1:2.

produced. Surface morphology of different ratios of starch–Aam complexes showed that the amount of starch used directly affected the porosity of the hydrogels (Figure 3(a) to (c)). As can be

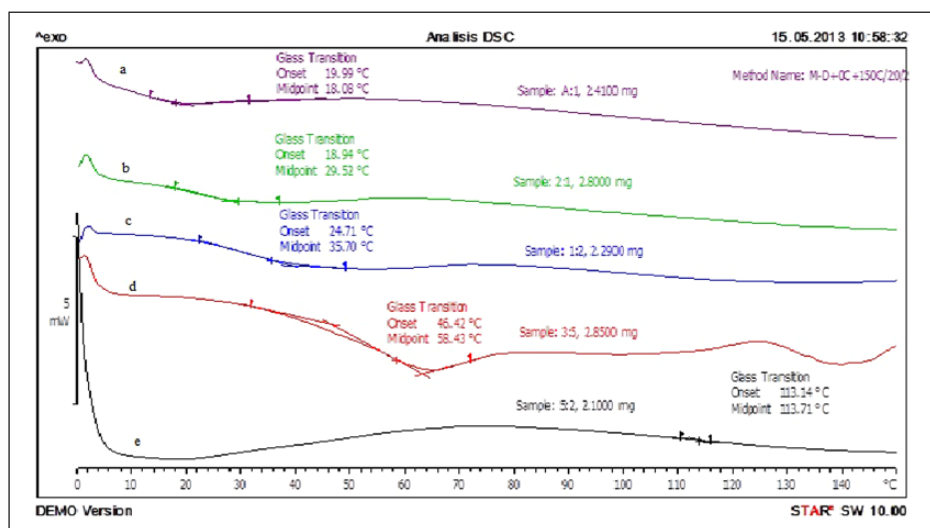


**Figure 4.** DSC thermograms of different ratios of the hydrogels: (a) starch powder, (b) hydrogel ratio 2:1, (c) hydrogel ratio 1:2, (d) hydrogel ratio 3:5, and (e) hydrogel ratio 5:2.

seen, the hydrogel with a ratio of 3:5 gave the most porous structure compared to the hydrogel with a higher amount of pAam (Figure 3(b)). A quick test has been applied to all samples by placing them in an aqueous medium. After being left for about 15 min, all samples swelled to twice its initial size. Hence, the porosity has affected the rate of absorbance of the hydrogels. This will be discussed in the next section.

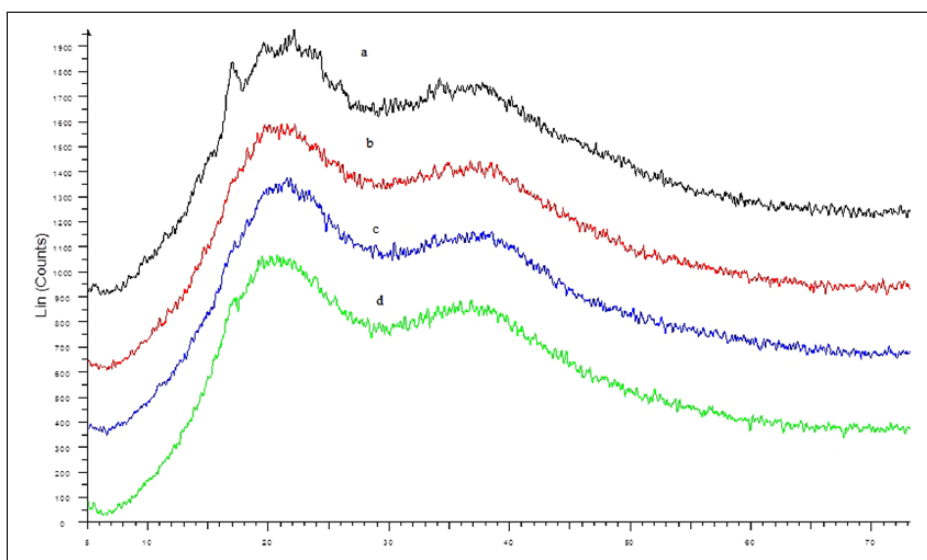
## DSC

Figure 4 shows the DSC analysis of starch and S-g-pAam hydrogels at different ratios a (starch), b (2: 1), c (1: 2), d (3:5), and e (5:2). It was noted that the differences in starch and monomer ratios significantly influenced the glass transition temperature ( $T_g$ ) of the hydrogels. The observation that all S-g-pAam hydrogels have a 4% weight loss below 10°C suggested the loss of absorbent and bound water in the hydrogel network. As the temperature increased from 20°C to 30°C, all hydrogels significantly increased the amount in weight lost with sample (b) 12.5% at 29.52°C, (c) 13.4% at 35.70°C, and (d) 30.3% at 58.43°C, respectively. These results indicate that many complicated processes occurred including the dehydration of carbohydrate chains and the breaking of C–O–C glycosidic bonding of the starch chain. However, there was prominent difference in the transitional glass temperature between the grafted hydrogels and starch. It has a higher temperature range compared to the original starch ( $T_g$ ) which is 18.08°C, whereas the grafted hydrogel showed  $T_g$  in the range of 29.50°C–58.40°C. The grafted hydrogels (S-g-pAam) were thermally stable which coincided with the amount of starch that existed in the networks. On the other hand, the starch not only strengthens the networks but also acts as a heat barrier, thus enhancing the thermal stability of the hydrogels.

## XRD

The XRD patterns of synthesized hydrogels and overall XRD results are shown in Figure 5. The starch diffractogram showed only one strong diffraction peak which was observed at  $2\theta = 18.0^\circ$





**Figure 5.** XRD diffractogram of the hydrogels S-g-pAam with various ratios at  $2\theta$  scale: (a) starch powder; (b, c, and d) starch-grafted polyacrylamide with various ratios 2:1, 1:2, and 3:5.

where it resembled the characteristic  $\beta$ -type crystalline structure.<sup>40</sup> It is noted that starch exists in a semi-crystalline in nature with regard to the amylopectin and amylose portion. Both compounds have typical crystalline peaks that appear at about  $16.6^\circ$  and  $22.0^\circ$  due to its close molecular packing and regular crystallization.<sup>30</sup> pAam has shown intense peaks at  $2\theta = 38.9^\circ$ . Based on the demonstrated X-ray diffractograms of hydrogels, it was an amorphous compound with intense peaks at approximately  $20.0^\circ$ , thus indicating that the crystallinity of the membranes was mainly contributed to by the monomer.<sup>41,42</sup>

### Swelling behavior

In previous sections, the surface morphology and hydrogel porosity have been discussed. It was noted that a high swelling ratio is related to the formation of vastly porous structures, consequently increasing the transparency of hydrogels.<sup>43</sup> According to the Flory–Huggins–Tanaka theory, the swelling ability of hydrogels is controlled by the amount of carboxyl group.<sup>44</sup> Furthermore, the capability of hydrogels is also related to the amount of monomer or comonomer used. As an example, a mole of pAam contains 1 mole of ionic unit ( $-\text{COOH}-$ ). Hence, the equilibrium swelling hydrogels increased significantly with the content of Aam-used S-g-pAam hydrogels in this research.

The results of equilibrium swelling times of the hydrogels at ultra pure water and citric acid–phosphate solutions of definite pH values are represented in Figure 6. S-g-pAam hydrogel (1:2, 2:1, and 3:5) were immersed in different pH solutions. The swollen hydrogels were taken out at timed intervals and superficially dried with filter paper before weighing. Then, the hydrogels were immersed again in the pH solutions followed by drying and weighing as described above within 60 min. The measurements were continued until a constant weight was reached for each hydrogel sample. Inspection of the equilibrium times revealed a result of approximately 7 in pure water; similar results were collected at pH 1 and 13.

During the pH-dependent swelling experiments, the hydrogel of ratio 2:1 swelled to approximately 84% in pure water. For pH 1 and 13, hydrogels swelled the highest at approximately 100%

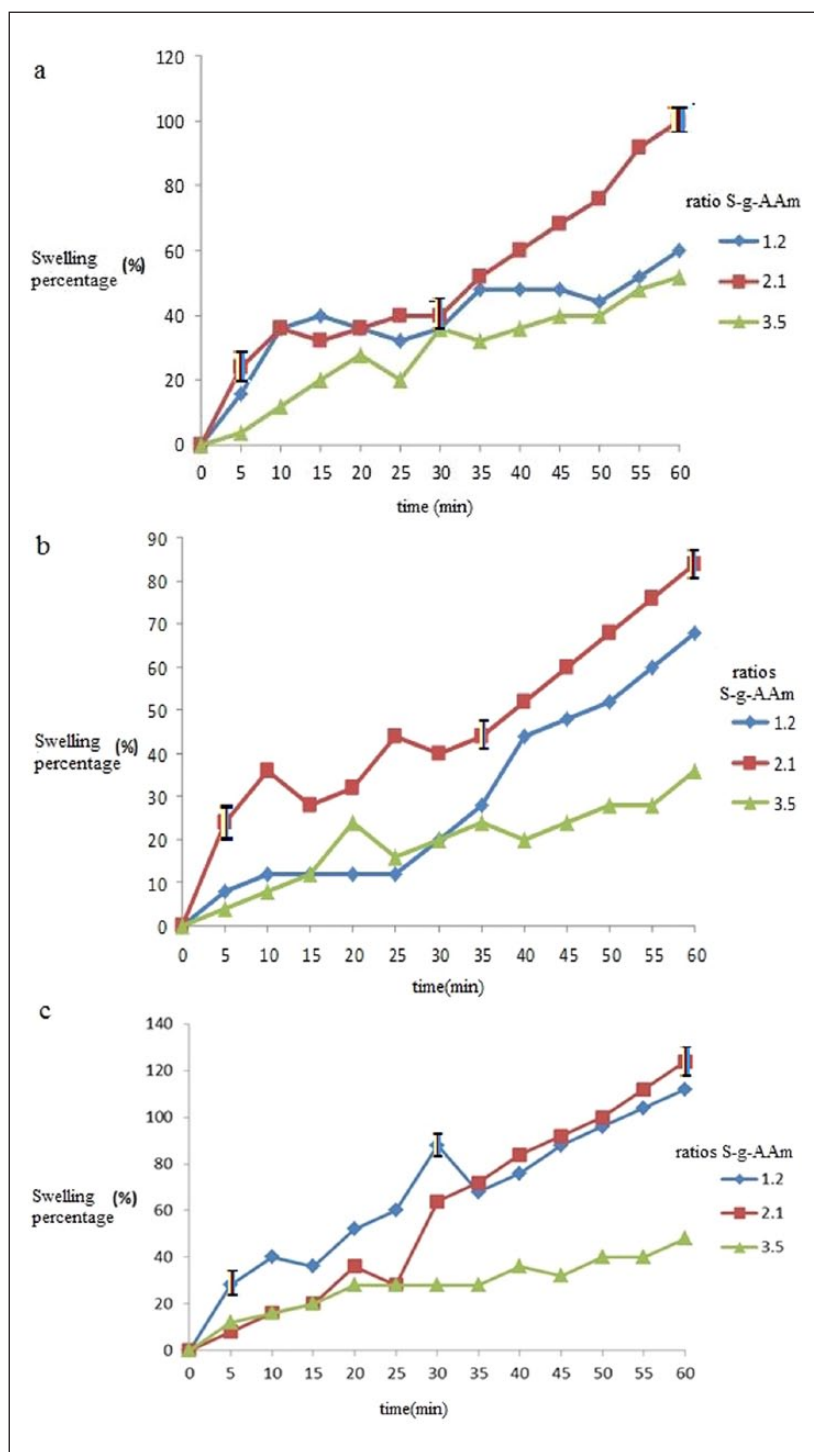


**Figure 6.** Equilibrium swelling times for grafted hydrogel S-g-pAam as a function of pH: (a) pH 1, (b) pH 7, and (c) pH 13.

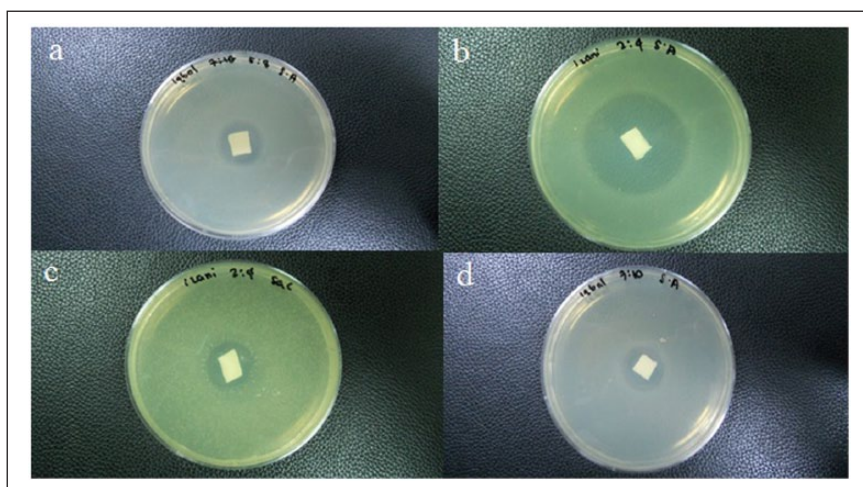


**Figure 7.** Antibacterial test for several ratios of grafted hydrogels (S-g-pAam): (a) *S. aureus* 3:5, (b) *S. aureus* 1:2, (c) *S. cerevisiae*, and (d) *E. coli* 5:3.

and 124%, respectively, at ratio 2:1. When the samples were immersed in the citric acid–phosphate solutions of different pH values and left in each solution for a maximum of 1 h, there were remarkable changes observed on the swelling ratio for all the hydrogels. These results denoted that the swelling behaviors of the hydrogels were essentially dependent on the pH of the varied solutions. As starch and Aam contained ionizable functional groups, this result was compatible with the expected values.

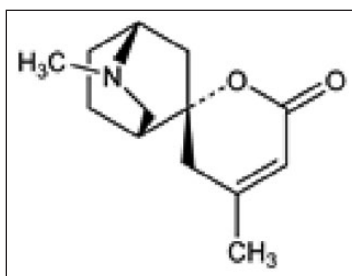
At a higher pH (13), the increasing amount of ionized groups has caused the generation of electrostatic repulsion forces among the adjacent ionized groups of the polymer networks. Hence, it has resulted in network expansion and a large volume of the hydrogel structure consisting of aqueous solution. Meanwhile, at a lower pH of 2 (below pKa), the carboxyl groups of the hydrogels are protonated and the competition of cations with the binding sites in the absorbents resulted in very low uptake capability. The absorption capacity of hydrogels in neutral buffer solution was 12% lower than in distilled water. The inefficient water uptake suggests that ionic strength also plays an important role for the absorbency ability. Moreover, the presence of inorganic electrolytes in a liquid contributes to the osmotic pressure difference between hydrogels' polymeric networks and the external solution. This effect may also lead to an intense shrinkage of the porous hydrogels. As a result, the amount of absorption has decreased sharply.

### Antibacterial efficiency test

An antibacterial efficiency test was carried out to determine inhibitory activity of starch–pAam (S-g-pAam), and it was measured based on the comparison between growth conditions of *E. coli* sp., *S. aureus*, *S. cerevisiae*, and *Salmonella typhi*. If all the bacteria around the plate grow in the same scale, it is assumed that no inhibition has occurred. The results presented in Figure 7 show that the area of inhibition of bacteria around the sample hydrogel was recorded. After growing for 24 h in the culture medium, a large amount of bacteria have covered the bottom of the culture disk except where the S-g-pAam membrane existed (Figure 7). Thus, it can be concluded that S-g-pAam hydrogel has an outstanding antibacterial activity because of the absence of clear hollow on

**Table 1.** Disinfection activity of synthesized hydrogels as a function of different pathogenic microbes.

Tested organisms/ hydrogel sample	Zones of inhibition (+/–)		
	2:1	1:2	3:5
<i>E. coli</i>	–	–	+
<i>S. aureus</i> (palm kernel)	–	+	+
<i>Salmonella typhi</i> .	–	–	+
<i>S. cerevisiae</i>	–	–	+

**Figure 8.** Chemical structure of “dioscorine” toxic alkaloids that are found in the *Dioscorea hispida* starch tuber.

the surface of the nutrient agar against various bacteria that were tested. As reported in previous research, antimicrobial activity was tested by measuring the turbidity of the medium. The disinfection activity of synthesized hydrogels is shown in Table 1.

Based on the results shown in Table 1, hydrogel at ratio 3:5 inhibits activity of all species of bacteria such as *E. coli*, *S. cerevisiae*, *S. aureus*, and *Salmonella typhi*. This may possibly be related to the existence of alkaloids in the yam, especially dioscorine (Figure 8) which gave highly remarkable disinfection effects (Figure 7). In general, dioscorine is part of a group of toxic alkaloids that contain large amounts of nitrogen. The presence of a cyclic chain with nitrogen bonding with the carbon group (C–N) gives antioxidant ability, including antibacterial properties against certain bacterial species.<sup>45</sup>

### Toxicity test by using zebrafish embryo test (FET)

Figure 9–11 are representative images of fish embryo toxicity tests of three different starch hydrogel extracts. Toxicity of the extracts were evaluated at 24, 48, 72, and 96 hours post fertilization (hpf). The dead embryos are represented by red color (labeled as D), survived embryos by blue color (labeled as S) while hatched embryos by green color (labeled as H). Figure 12 shows the percentage of survival embryos against different dilutions of starch extracts (2:1). At the end of 96 hpf, no embryos survived in raw dilution. The percentage of survival embryos for 1:10, 1:100, 1:1000, and 1:10,000 are 66.67%, 77.78%, 77.78%, and 88.89%, respectively. Therefore, embryos can survive in the starch hydrogel extract with minimum of at least 10× dilutions.

Figure 10 shows the condition of zebrafish embryos at different concentrations of PAam:starch extract ratio (1:2) at 24, 48, 72, and 96 hpf. The red color indicates dead embryos while the blue color

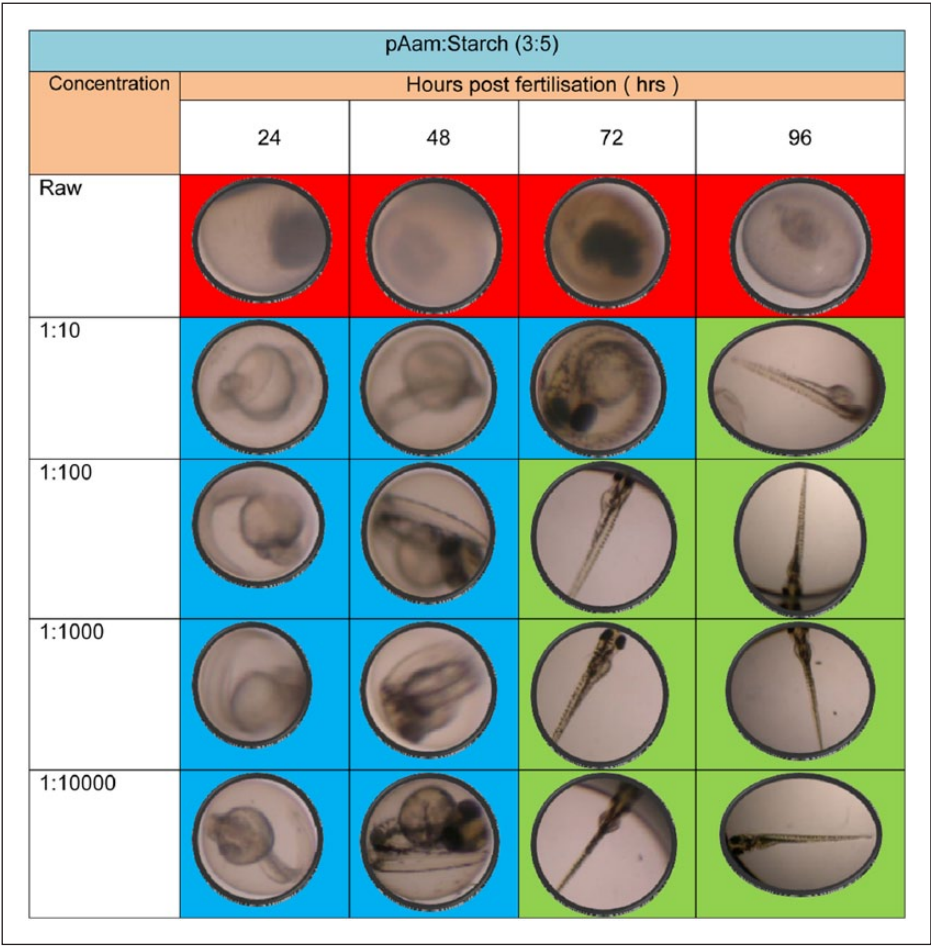


**Figure 9.** Zebrafish embryo post-fertilization until 96 h at pAam:starch (3:5) hydrogel extract.

indicates the survival of embryos. The green color shows the embryos that have hatched. Figure 12 shows percentage of survival embryos against different concentrations of starch (1:2). At the end of 96 hpf, no embryos survived in raw starch (1:2) hydrogel extract. The percentage of survival embryos for 1:10, 1:100, 1:1000, and 1:10000 are 55.56%, 88.89%, 77.78%, and 88.89%, respectively. Therefore, embryos can survive in the starch (1:2) hydrogel extract with at least 10× dilution.

Based on Figure 12, all undiluted 3:5, 1:2, and 2:1 pAam–starch extracts caused all the embryos to die after 96 hpf, which suggests that the starch from *D. hispida* sp. is toxic to the embryos. In the 1:100 test solution, the embryos did not survive after 96 h, although based on observations, the embryos initially displayed some level of development before dying. The 1:1000 and 1:10,000 dilute extract tests show all the embryos, including the replicates, survived at the end of the 96-h observation. All the embryos showed normal development and showed no indication of deformation.

The 1:2 pAam–starch stock solution gave the highest embryo survival rate in comparison with 2:1 and 3:5 solutions; 0% of the embryos survive after 96-h exposure to the undiluted solution, while 88.89%, 77.89%, and 88.89% embryos exposed to 1:100, 1:1000, and 1:10,000 test solutions



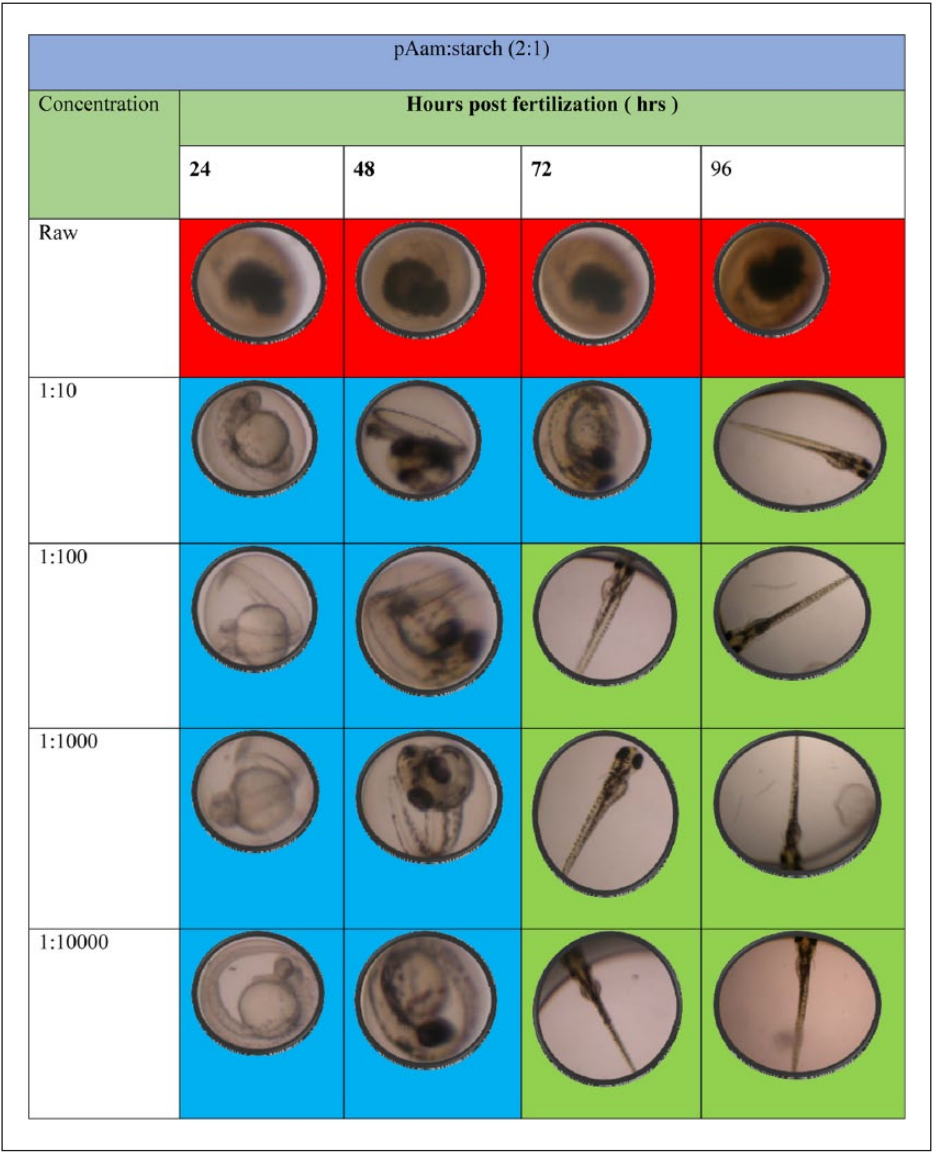


**Figure 10.** Zebrafish embryo post-fertilization until 96 h in pAam:starch (2:1) hydrogel extract.

survived after 96 h of observation. The embryos were developing normally and displayed no signs of deformation that could be caused by the test solutions. However, it should be pointed out that these data might not be fully representative, as the sample size of the experiment was limited.

**Conclusion**

S-g-pAam hydrogels were synthesized using *N,N'*-MBA as a cross-linking agent and their in vitro antimicrobial activities with toxicity tests using FET assay were investigated. No bands in the FTIR spectrum of the hydrogels significantly differed from the bands corresponding to their individual



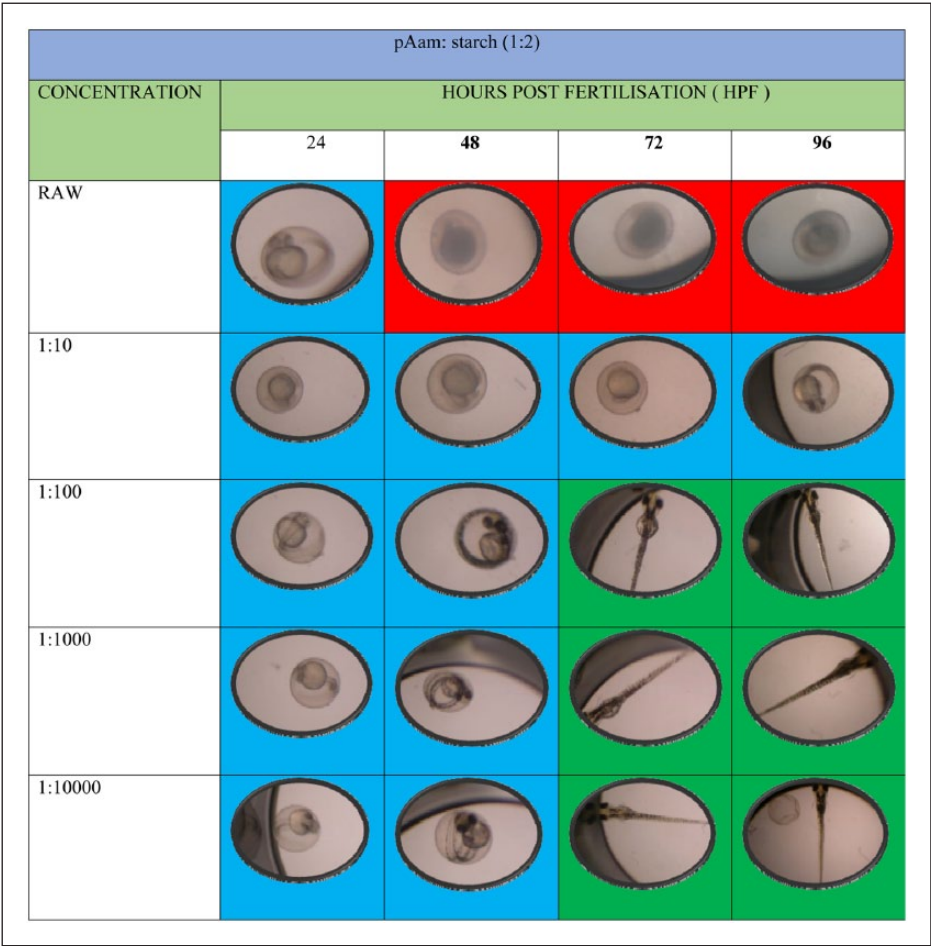


**Figure 11.** Zebrafish embryo post-fertilization until 96 h in pAam:starch (1:2) hydrogel extract.

components. This result shows that the functional groups in the structure of starch and pAam did not change significantly, as the stretch band corresponding to cross-linking of starch and pAam was expected at  $1642\text{ cm}^{-1}$ . DSC curves showed that the thermal stability of starch–pAam hydrogels was directly proportional to the increasing amount of starch as a result of modification processes. X-ray diffractograms of the hydrogels revealed amorphous compounds, with intense peaks at approximately  $2\theta=20.0^\circ$ , which suggest that the crystallinity imparted in the hydrogels is mainly due to crystallinity of starch and pAam. The swelling behaviors of the hydrogels were found to be pH dependent due to ionizable functional groups within the pAam. In this study we also show that the hydrogel at 3:5 pAam:starch ratio has a remarkable antimicrobial activity against *E. coli*., *S. aureus*., *S. cerevisiae*, and *Salmonella typhi*. For further applications, the starch from this yam tuber can be developed as a universal, microbial resistant coating for wood stocks, fruits, metals and many other surfaces. The dioscorine within the tuber’s starch would protect the coated materials from rotting by bacteria or fungi activity. We also demonstrated that this starch could be developed into a starch-based superabsorbent. To conclude, the formulation for developing hydrogels in this study especially the 2:1 pAam:starch ratio, shows an acceptable level of toxicity and thus compatible for biological applications.

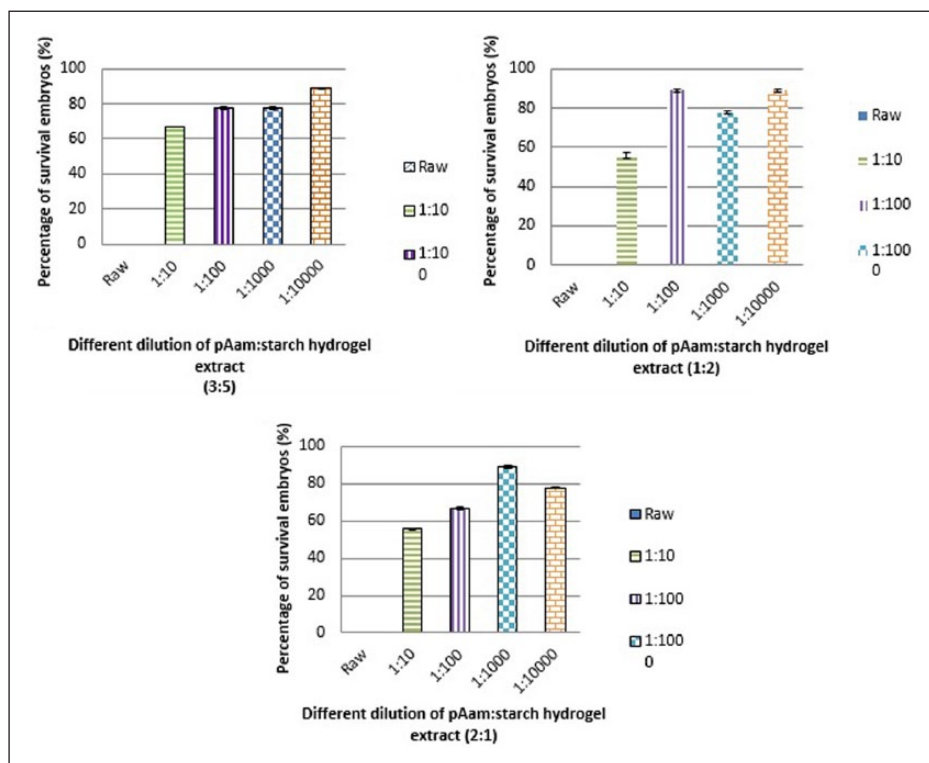


**Figure 12.** Percentage of toxicity level of pAam:starch at varied ratios of polyacrylamide and starch (1:2, 2:1, and 3:5).

### Declaration of conflicting interests

The authors declared no potential conflicts of interest with respect to the research, authorship, and/or publication of this article.

### Funding

This work was financially supported, in part, by research grants FRGS/1/2014/ST01/UKM/03/1, GUP-2014-079, ERGS/1/2012/STG05/UKM/03/2, and DIP-2014-016 given by Universiti Kebangsaan Malaysia and the Ministry of Education.

### References

1. Athawale VD and Lele V. Recent trends in hydrogels based on starch-graft-acrylic acid: a review. *Starch/Stärke* 2001; 53: 7–13.
2. Cao LQ, Xu SM and Feng S. Swelling and thermal behaviors of a starch-based superabsorbent hydrogel with quaternary ammonium and carboxyl groups. *J Appl Polym Sci* 2005; 96: 2392–2398.
3. Lee JS, Kumar RN, Rozman HD, et al. Pasting, swelling and solubility properties of UV initiated starch-graftpoly(AA). *Food Chem* 2005; 91: 203–211.
4. Tong QY and Zhang GW. Rapid synthesis of a superabsorbent from a saponified starch and acrylonitrile/AMPS graft copolymers. *Carbohydr Polym* 2005; 62: 77–84.
5. Kulkarni RV and Biswanath Sa. Electroresponsive polyacrylamide-grafted-xanthan hydrogels for drug delivery. *J Bioact Compat Pol* 2009; 24(4): 368–384.
6. Hosseinzadeh H, Pourjavadi A, Mahdavinia GR, et al. Modified carrageenan. 1. H-CarragPAM, a novel biopolymer-based superabsorbent

- hydrogel. *J Bioact Compat Pol* 2005; 20(5): 475–490.
7. Wu JH, Lin JM, Zhou M, et al. Synthesis and properties of starch-graft-polyacrylamide/clay superabsorbent composite. *Rapid Comm* 2000; 21: 1032.
8. Lu S, Lin T and Cao D. Inverse emulsion of starch-graft-polyacrylamide. *Starch/Stärke* 2003; 55: 222–227.
9. Yeng WS, Tahir PM, Chiang LK, et al. Sago starch & its acrylamide modified products as coating material on handsheets made from recycled pulp fibers. *J Appl Polym Sci* 2004; 94: 154.
10. Deshmukh SR, Sudhakar K and Singh RPJ. Drag- reduction efficiency, shear stability and biodegradation resistance of carboxymethyl cellulose-based and starch-based copolymers. *Appl Polym Sci* 1991; 43: 1091–1101.
11. Hebeish A, El-Raffie MH, Higazy A, et al. Synthesis, characterization and properties of polyacrylamide–starch composites. *Starch/Stärke* 1996; 48: 175–179.
12. Fanta GF. Starch graft copolymers. *Polymerization of Mathematical Engineering* 10; 7901–7910.
13. Zhang JP, Li A and Wang AQ. Study on superabsorbent composite, VI. Preparation, characterization and swelling behaviors of starch phosphate-graft-acrylamide/attapulgit superabsorbent composite. *Carbohydr Polym* 2006; 65: 150–158.
14. Li A, Zhang JP and Wang AQ. Utilization of starch and clay for the preparation of superabsorbent composite. *Bioresource Technol* 2007; 98: 327–332.
15. Chen J and Park K. Synthesis and characterization of superporous hydrogel composites. *J Control Release* 2000; 65: 73.
16. Hron P, Šlechtová JS, Smetana K, et al. Silicone rubber-hydrogel composites as polymeric biomaterials, IX. Composites containing powdery polyacrylamide hydrogel. *Biomaterials* 1997; 18: 1069–1073.
17. Nashriyah M, Nornasuh Y, Salmah T, et al. *Dioscorea hispida* dennst. (dios-coreaceae): an overview. Buletin UniSZA, No. 4, 2010: ISSN 2180-0235.
18. Tattiyakul J and Naksriarporn T. X-ray diffraction pattern and functional properties of *dioscorea hispida* dennst starch hydrothermally modified at different temperatures. *Food Bioprocess Tech* 2010. Doi: 10.1007/s11947-010-0424.
19. Udensi EA, Oselebe HO and Iweala OO. The investigation of chemical composition and functional properties of water yam (*Dioscorea alata*): effect of varietal differences. *Pakistan J Nutr* 2008; 7(2): 324–344.
20. Hudzari RM, Ssomad MAHA, Rizuwan YM, et al. Development of automatic alkaloid removal system for *Dioscorea hispida*. *Front Sci* 2011; 1(1): 16–20.
21. Hudzari RM, Muhammad HH, Mohd NA, et al. A review on farm mechanization and analysis aspect for *Dioscorea hispida*. *J Crop Sci* 2000; 2(1): 21–26.
22. Hahn SK. Yams: *Dioscorea* spp. (Dioscoreaceae). In: Smartt J and Simmonds NW (eds) *Evolution of crop plants*. Harlow: Longman Scientific & Technical, 1995, pp. 112–120.
23. Abdullah Salam A. *Poisonous plants of Malaysia*. 1st ed. Kuala Lumpur, Malaysia: Tropical Press Sdn Bhd, 1990, p. 19.
24. Agbor-Egbe T and Treche S. Evaluation of chemical composition of Cameroonian yam germplasm. *J Food Compos Anal* 1995; 8: 274–283.
25. Yan X and Gemeinhart RA. Cisplatin delivery from poly(acrylic acid-co-methyl methacrylate) microparticles. *J Control Release* 2005; 106: 198–208.
26. Cairns P, Sun L, Morris VJ, et al. Physicochemical studies using amylose as an in vitro model for resistant starch. *J Cereal Sci* 1995; 21: 37–47.
27. Singh OP, Sandle NK and Varma IK. Graft-copolymerization of starch with acrylamide, II. Thermal behavior of graft copolymers. *Angew Makromol Chem* 1984; 121: 187–193.
28. Okwu DE and Ndu CU. Evaluation of the phytonutrients, mineral and vitamin contents of some varieties of yam (*Dioscorea* sp.). *Int J Mol Med Adv Sci* 2006; 2(2): 199–203.
29. Poornima GN and Ravishankar Rai V. Evaluation of phytochemicals and vitamin contents in a wild yam, *Dioscorea belophylla* (prain) Haine. *Afr J Biotechnol* 2009; 8(6): 971–973.
30. Ayyanar M and Ignacimuthu S. Ethnomedicinal plants used by the tribals of Tirunelveli hills to treat poisonous bites and skin diseases. *Indian J Tradit Know* 2005; 4: 229–236.
31. Airul Ashri M, Sukeri M, Yusof M, et al. Physicochemical characterization of starch extracted from Malaysian wild yam (*Dioscorea hispida* Dennst). *Emir J Food Agric* 2014; 26(8): 652–658.

32. Clark CL, Jacobs MRJ and Appelbaum PC. Antipneumococcal activities of levofloxacin and clarithromycin as determined by agar dilution, microdilution, E-test, and disk diffusion methodologies. *J Clin Microbiol* 1998; 36(12): 3579–3584.
33. Leung L and Holt CE. Imaging axon pathfinding in zebrafish in vivo. *Cold Spring Harb Protoc* 2012; 9: 992–997.
34. Organization for Economic Cooperation and Development (OECD). *Draft proposal for a new guideline—Fish Embryo Toxicity (FET) test: draft guideline*. Paris: OECD, 2006.
35. Organization for Economic Cooperation and Development (OECD). *Draft proposal for a new guideline—Fish Embryo Toxicity (FET) test: draft guideline*. Paris: OECD, 2013.
36. Russell SM, Belcher EB and Carta G. Protein partitioning and transport in supported cationic acrylamide-based hydrogels. *AIChE J* 2003; 49: 1168.
37. Swatschek D, Schatton W, Muller WEG, et al. Microparticles derived from marine sponge collagen (SCMPs): preparation, characterization and suitability for dermal delivery of all-trans retinal. *Eur J Pharm Biopharm* 2002; 54: 125–133.
38. Nagasawa N, Yagi T, Kume T, et al. Radiation crosslinking of carboxymethyl starch. *Carbohydr Polym* 2004; 58: 109–113.
39. Pal K, Banthia AK and Majumdar DK. Preparation and characterization of polyvinyl alcohol–gelatin hydrogel membranes for biomedical applications. *AAPS Pharm Sci Tech* 2007; 8(1): E1–E5.
40. Ichikawa H, Arimoto M and Fukumori Y. Design of starch based microcapsules with hydrogel as a membrane component and their preparation by a spouted bed. *Powder Technol* 2003; 130: 189.
41. Singh V, Tiwari A, Sadan P, et al. Microwave-accelerated synthesis and characterization of potato starch-g-poly(acrylamide). *Starch/Stärke* 2006; 58: 536–543.
42. Lopour P, Plichta Z, Volfová Z, et al. Silicone rubber–hydrogel composites as polymeric biomaterials, IV. Silicone matrix-hydrogel filler interaction and mechanical properties. *Biomaterials* 1993; 14: 1051–1055.
43. Theis T and Stahl U. Antifungal proteins: targets, mechanisms and prospective applications. *Cell Mol Life Sci* 2004; 61: 437–455.
44. Ludwig A. The use of mucoadhesive polymers in ocular drug delivery. *Adv Drug Deliv Rev* 2005; 57: 1595–1639.